Structural Engineering and Mechanics, *Vol. 59, No. 6 (2016) 1139-1153*
DOI: http://dx.doi.org/10.12989/sem.2016.59.6.1139

Effects of deformation of elastic constraints on free vibration characteristics of cantilever Bernoulli-Euler beams

Tong Wang[1a], Tao He[*1,2] and Hongjing Li[3b]

[1]*College of Civil Engineering, Shanghai Normal University, Shanghai, 201418, China*
[2]*School of Civil Engineering, University of Birmingham, Birmingham, B15 2TT, UK*
[3]*College of Civil Engineering, Nanjing Tech University, Nanjing, 211816, China*

(Received January 30, 2016, Revised June 2, 2016, Accepted June 10, 2016)

Abstract. Elastic constraints are usually simplified as "spring forces" exerted on beam ends without considering the "spring deformation". The partial differential equation governing the free vibrations of a cantilever Bernoulli-Euler beam considering the deformation of elastic constraints is firstly established, and is nondimensionalized to obtain two dimensionless factors, κ_v and κ_r, describing the effects of elastically vertical and rotational end constraints, respectively. Then the frequency equation for the above Bernoulli-Euler beam model is derived using the method of separation of variables. A numerical analysis method is proposed to solve the transcendental frequency equation for the continuous change of the frequency with κ_v and κ_r. Then the mode shape functions are given. Finally, effects of κ_v and κ_r on free vibration characteristics of the beam with different slenderness ratios are calculated and analyzed. The results indicate that the effects of κ_v are larger on higher-order free vibration characteristics than on lower-order ones, and the impact strength decreases with slenderness ratio. Under a relatively larger slenderness ratio, the effects of κ_v can be neglected for the fundamental frequency characteristics, while cannot for higher-order ones. However, the effects of κ_r are large on both higher- and lower-order free vibration characteristics, and cannot be neglected no matter the slenderness ratio is large or small.

Keywords: deformation; elastic constraint; free vibration characteristic; cantilever beam; Bernoulli-Euler beam; frequency equation; mode shape function

1. Introduction

Owing to its extensive application in engineering, the transversely vibrating beam has been a hot research topic in the field of engineering mechanics for the past more than one century (Timoshenko 1953, Thomson and Dahleh 1997). With deepening of the research, the beam theory has been being improved gradually, successively from the Bernoulli-Euler to Rayleigh, shear and Timoshenko, more and more accurate and close to reality (Traill-Nash and Collar 1953, Han *et al.* 1999). And more recently, Plankis *et al.* (2015) proposed a three-dimensional elasticity-based

∗Corresponding author, Ph.D., E-mail: taohe@shnu.edu.cn
[a]Ph.D., E-mail: tongwang@shnu.edu.cn
[b]Professor, E-mail: harbiner@163.com

http://www.techno-press.org/?journal=sem&subpage=8 ISSN: 1225-4568 (Print), 1598-6217 (Online)

beam theory in which a few of the assumptions included in the above four beam theories are removed, closer to reality. Liang *et al.* (2014) established a new Bernoulli-Euler beam model based on a simplified strain gradient elasticity theory, and discussed the influences of Poisson's effect as well as the weak non-local strain gradient elastic effect. So far, there still exists some certain discrepancy between the beam theory and engineering practice. Two key factors contribute to it. The first and most concerned one is the approximation degree of the beam theory itself, while the other is the reasonableness of the adopted boundary conditions, which is often less concerned or even ignored.

In most previous studies on transverse vibrations of beams, end supports are usually simplified as rigid constraints, neglecting the elasticity of end supports, which is undoubtedly convenient for establishing and analyzing the beam theory, while may bring errors or mistakes in some cases. As is known to all, all structural materials possess to some extent elasticity. So only when the stiffness of end supports is much larger than that of the beam can the assumption of rigid constraint be reasonable. However, in practice, this requirement usually cannot be satisfied very well, for example, a girder bridge with highly flexible piers (Wang *et al.* 2015) and a submarine pipeline laid on a soft seabed (Choi 2001), for which the elasticity of end supports has to be considered. Till now, a considerable amount of research has been performed on vibration analysis of beams with elastic supports. Chun (1972) derived exact expressions for the natural frequencies and mode shapes of a beam with one end spring-hinged and the other end free. Maurizi *et al.* (1976) studied the free vibration of a uniform beam with one end hinged and rotationally restrained, and the other end restrained by a transverse spring. Afolabi (1986) analyzed the effects of the rotational and transversal support flexibility on the natural frequency of an almost clamped-clamped beam and a flexibly supported cantilever beam. Lee and Ke (1990) studied the free vibration of an elastically restrained symmetric non-uniform Timoshenko beam resting on a non-uniform elastic foundation and subjected to an axial load. Rao and Mirza (1989) and Li (2000) studied analytically the free vibration of beams restrained by two transverse springs and two rotational springs. Xing and Wang (2013) gave the frequency equations and shape functions for the beams with two transversal and two rotational elastic springs subjected to a constant axial load. Duy *et al.* (2014) studied the free vibration of functionally graded material beams on an elastic foundation and spring supports. Shi *et al.* (2014) reported the effects of elastic supports and added masses on dynamic characteristics of a three-span non-uniform beam bridge. In addition, there are many other related studies which are regrettably omitted here.

Among the above studies on vibrating beams with elastic end supports exists a common point that the elastic end constraints are usually simplified as "spring force" exerted on beam ends, ignoring the "spring deformation" which may be unreasonable in practice. Wang *et al.* (2015) derived the governing equation of motion for a hinged-hinged Bernoulli-Euler beam under vertical ground motion considering elastically vertical deformation of end supports, and found that elastic end supports may magnify or minify vertical seismic responses of the beam. So it is very necessary to study the effects of elastic end supports (including their deformation) on dynamic characteristics of the beam. In this paper, we extend the study of Wang *et al.* (2015), and consider the free vibrations of cantilever Bernoulli-Euler beams with elastic constraints. In the next section, the dimensionless governing equation of motion for a uniform Bernoulli-Euler beam with one end elastically constrained and the other free is derived in detail, in which there are two dimensionless factors, κ_v and κ_r, describing the effects of the elastically vertical and rotational constraints, respectively. Then the frequency equation for the above beam model is derived in Section 3 using the method of separation of variables. Section 4 presents a numerical analysis method to solve the

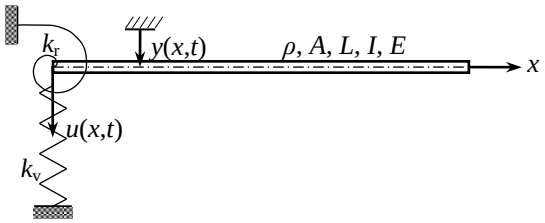

Fig. 1 A uniform cantilever Bernoulli-Euler beam with elastic constraints

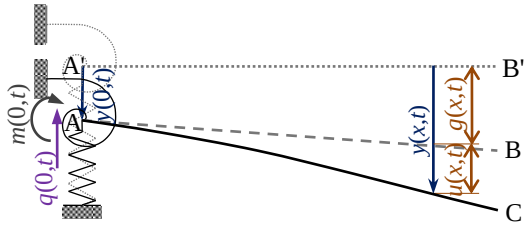

Fig. 2 Vertical displacements of the cantilever Bernoulli-Euler beam with elastic constraints

obtained frequency equation for the continuous change of the frequency with κ_v and κ_r. Then the mode shape functions corresponding to the calculated frequencies are given in Section 5. Section 6 calculates and analyzes the effects of κ_v and κ_r on free vibration characteristics of the beam under different slenderness ratios. Finally, some conclusions are summarized in Section 7.

2. Equation of motion and boundary conditions

Fig. 1 shows a beam with one end elastically supported and the other end free to be considered in this study, in which the density ρ, the span L, the section area A, the area moment of inertia I and the elastic modulus E are all constants. Both the vertical and rotational displacements of the left end are elastically constrained, and accordingly k_v and k_r are the vertical and rotational constraint stiffness, respectively.

The coordinate system adopted is also shown in Fig. 1, in which the x axis is defined as the central axis of the beam at its original (or static) position, $y(x,t)$ is the absolute displacement of the beam relative to the x axis, and $u(x,t)$ is the displacement relative to the rigid central axis, i.e., the deformation from the broken line AB to the curve AC as shown in Fig. 2. The dotted line A'B' is the original (static) position of the beam, while the curve AC is the final position. The broken line AB is the position of the rigid beam due to the deformation of elastic constraints, and the rigid body displacement from the dotted line A'B' to the broken line AB is denoted as $g(x,t)$. All displacements are supposed to be elastic and linear to satisfy the superposition principle, i.e., the assumption of small displacement, and $y(x,t)$ and $u(x,t)$ can both be considered vertical based on this assumption.

From Fig. 2, the total (absolute) displacement $y(x,t)$ is equal to the flexural displacement $u(x,t)$ plus the rigid body displacement $g(x,t)$, i.e.

$$y(x,t) = u(x,t) + g(x,t) \tag{1}$$

The rigid body displacement $g(x,t)$ is determined by the left end displacements of the beam, i.e., the vertical displacement $y(0,t)$ and the rotational angle $\partial y(0,t)/\partial x$ (for simplicity $\partial y(0,t)/\partial x = \partial y(x,t)/\partial x|_{x=0}$). It can be calculated based on the superposition principle by

$$g(x,t) = y(0,t) + \frac{\partial y(0,t)}{\partial x} x \tag{2}$$

According to the action and reaction principle, the end shear $q(0,t)$ and moment $m(0,t)$ of the beam, as shown in Fig. 2, should equal the vertical and rotational constraint forces, respectively, i.e.

$$q(0,t) = k_{\mathrm{v}} y(0,t) \tag{3}$$

$$m(0,t) = -k_{\mathrm{r}} \frac{\partial y(0,t)}{\partial x} \tag{4}$$

in which

$$m(0,t) = -EI \frac{\partial^2 u(0,t)}{\partial x^2} \tag{5}$$

$$q(0,t) = \frac{\partial m(0,t)}{\partial x} = -EI \frac{\partial^3 u(0,t)}{\partial x^3} \tag{6}$$

Substituting Eqs. (3)-(6) into Eq. (2) and the resulting equation into Eq. (1) gives

$$y(x,t) = u(x,t) - \frac{EI}{k_{\mathrm{v}}} \frac{\partial^3 u(0,t)}{\partial x^3} + \frac{EI}{k_{\mathrm{r}}} \frac{\partial^2 u(0,t)}{\partial x^2} x \tag{7}$$

Without damping, the equation of motion governing free vibrations of the beam shown in Fig. 1 can be written as

$$\rho A \frac{\partial y^2(x,t)}{\partial t^2} + EI \frac{\partial^4 u(x,t)}{\partial x^4} = 0 \tag{8}$$

Substituting Eq (7) into Eq. (8) yields

$$\rho A \frac{\partial^2 u(x,t)}{\partial t^2} + EI \frac{\partial^4 u(x,t)}{\partial x^4} - \frac{\rho AEI}{k_{\mathrm{v}}} \frac{\partial^5 u(0,t)}{\partial x^3 \partial t^2} + \frac{\rho AEI}{k_{\mathrm{r}}} \frac{\partial^4 u(0,t)}{\partial x^2 \partial t^2} x = 0 \tag{9}$$

The boundary conditions for the cantilever Bernoulli-Euler beam are

$$u(x,t) = \frac{\partial u(x,t)}{\partial x} = 0, \quad x = 0 \tag{10}$$

$$\frac{\partial^2 u(x,t)}{\partial x^2} = \frac{\partial^3 u(x,t)}{\partial x^3} = 0, \quad x = L \tag{11}$$

For convenience, nondimensionalize $u(x,t)$ and x by L, and t by $t_0 = (\rho L^2/E)^{1/2}$, i.e.

$$\xi = \frac{x}{L}, \quad \tau = \frac{t}{t_0}, \quad U(\xi,\tau) = \frac{u(x,t)}{L} \tag{12}$$

Then Eqs. (9)-(11) become

$$s^2\ddot{U}(\xi,\tau) + U'''(\xi,\tau) - \kappa_v\ddot{U}'''(0,\tau) + \kappa_r s^2\ddot{U}''(0,\tau)\xi = 0 \tag{13}$$

$$U(\xi,\tau) = U'(\xi,\tau) = 0, \quad \xi = 0 \tag{14}$$

$$U''(\xi,\tau) = U'''(\xi,\tau) = 0, \quad \xi = 1 \tag{15}$$

Here the prime " ′ " and the over dot " · " represent differentiation with respect to the dimensionless coordinate ξ and to the dimensionless time τ, respectively, and

$$s = \sqrt{\frac{AL^2}{I}}, \quad \kappa_v = \frac{EA}{Lk_v}, \quad \kappa_r = \frac{EI}{Lk_r} \tag{16}$$

are all dimensionless factors not less than zero, in which s is the slenderness ratio, and κ_v and κ_r the stiffness factors controlling the effects of the elastically vertical and rotational constraints, respectively. Based on the assumption of small displacement, κ_v and κ_r cannot be very large.

Eqs. (13)-(15) are just the dimensionless free vibration equation and corresponding boundary conditions for the cantilever Bernoulli-Euler beam with elastic constraints.

3. Frequency equation

Using the method of separation of variables, $U(\xi,\tau)$ can be decomposed into a temporal function $T(\tau)$ multiplied by a spatial function $V(\xi)$, i.e.

$$U(\xi,\tau) = T(\tau)V(\xi) \tag{17}$$

Substituting Eq. (17) into Eq. (13) gives

$$\ddot{T}(\tau)\left[s^2V(\xi) - \kappa_v V'''(0) + \kappa_r s^2 V''(0)\xi\right] + T(\tau)V''''(\xi) = 0 \tag{18}$$

The above expression can be separated into two ordinary differential equations given by

$$\ddot{T}(\tau) + \omega^2 T(\tau) = 0 \tag{19}$$

$$V''''(\xi) - \omega^2\left[s^2V(\xi) - \kappa_v V'''(0) + \kappa_r s^2 V''(0)\xi\right] = 0 \tag{20}$$

in which ω is the dimensionless frequency, and accordingly the dimensional one is given by ω/t_0.

Then the boundary conditions of Eqs. (14) and (15) become

$$V(\xi) = V'(\xi) = 0, \quad \xi = 0 \tag{21}$$

$$V''(\xi) = V'''(\xi) = 0, \quad \xi = 1 \tag{22}$$

From Eq. (19), $T(\tau)$ is sinusoidal in time

$$T(\tau)=d_1\sin\omega\tau+d_2\cos\omega\tau \tag{23}$$

where d_1 and d_2 are constant coefficients.

From Eq. (20), $V(\xi)$ can be assumed as

$$V(\xi)=C(e^{\lambda\xi}+\kappa_{\mathrm{v}}r^2\lambda^3-\kappa_{\mathrm{r}}\lambda^2\xi) \tag{24}$$

in which C is a constant coefficient, e the Euler's constant, r=1/s, and λ the wave number.

When Eq. (24) is substituted into Eq. (20), in order to have a non-trivial solution, the wave number λ can be solved as

$$\lambda_1=\mathrm{i}a,\ \ \lambda_2=-\mathrm{i}a,\ \ \lambda_3=a,\ \ \lambda_4=-a \tag{25}$$

in which i=$(-1)^{1/2}$, a=$(s/\omega)^{1/2}$. The quantity a is 1/(2π) times the number of cycles in a beam length, so we call a the dimensionless wave number.

Then the general solution of $V(\xi)$ is given by

$$V(\xi)=\sum_{n=1}^{4}C_n(e^{\lambda_n\xi}+\kappa_{\mathrm{v}}r^2\lambda_n^3-\kappa_{\mathrm{r}}\lambda_n^2\xi) \tag{26}$$

Expressing the exponential function in the above equation in terms of sinusoidal and hyperbolic functions yields

$$V(\xi)=c_1\sin a\xi+c_2\cos a\xi+c_3\sinh a\xi+c_4\cosh a\xi-(c_1-c_3)\kappa_{\mathrm{v}}r^2a^3+(c_2-c_4)\kappa_{\mathrm{r}}a^2\xi \tag{27}$$

in which c_1=i(C_1−C_2), c_2=C_1+C_2, c_3=C_3−C_4, c_4=C_3+C_4.

Substituting Eq. (27) into the boundary conditions of Eqs. (21) and (22) yields a system of liner algebraic equations, i.e.

$$\begin{bmatrix}-\kappa_{\mathrm{v}}r^2a^3 & 1 & \kappa_{\mathrm{v}}r^2a^3 & 1\\ 1 & \kappa_{\mathrm{r}}a & 1 & -\kappa_{\mathrm{r}}a\\ -\sin a & -\cos a & \sinh a & \cosh a\\ -\cos a & \sin a & \cosh a & \sinh a\end{bmatrix}\begin{Bmatrix}c_1\\c_2\\c_3\\c_4\end{Bmatrix}=\begin{Bmatrix}0\\0\\0\\0\end{Bmatrix} \tag{28}$$

The determinant of the matrix in Eq. (28) has to be zero to avoid the trivial solution, that is

$$\begin{aligned}&(1+\cos a\cosh a)-\kappa_{\mathrm{v}}r^2a^3(\sin a\cosh a+\cos a\sinh a)\\&-\kappa_{\mathrm{r}}a(\sin a\cosh a-\cos a\sinh a)+\kappa_{\mathrm{v}}\kappa_{\mathrm{r}}r^2a^4(1-\cos a\cosh a)=0\end{aligned} \tag{29}$$

Eq. (29) is just the frequency equation for the cantilever Bernoulli-Euler beam considering the deformation of elastic constraints. Clearly, the frequency equation contains four parts: the first term on the left-hand side is the frequency equation of the cantilever beam with rigid constraints, the second term the correction induced solely by the vertical constraint, the third term the correction induced solely by the rotational constraint, and the fourth term the mixed correction induced by both constraints.

4. Solution method for the frequency equation

So far, we have obtained the frequency equation for the cantilever beam with elastic constraints. Solving the frequency equation will yield the natural frequencies. However, it is much easier to directly obtain the dimensionless wave number a from Eq. (29) than to obtain the dimensionless frequency ω. Because a^2 is equal to the dimensionless frequency ω multiplied by the dimensionless slenderness ratio s, i.e., $a^2=s\omega$, a can also be called the "dimensionless frequency" (Kang 2014) or "frequency factor" (Ozturk and Coskun 2013). For simplicity, we just study in this paper the wave number a rather than the frequency ω. And ω can be calculated from the obtained wave number using the relationship, $\omega=a^2/s$.

Clearly, when the slenderness ratio s (or its reciprocal r) is given, Eq. (29) is a function of the wave number a and the stiffness factors κ_v and κ_r, or in other words, a is a function of κ_v and κ_r if s is given. Our primary goal in this paper is just to study the effects of κ_v and κ_r on the frequency ω or wave number a. The best way to represent the solution of the wave number is to plot wave numbers as a continuous function of κ_v and κ_r. However, the frequency equation (29) is a transcendental equation that has to be solved numerically, by such as the bisection or iterative method Faires and Burden 2012. In order to obtain a smooth function, $a(\kappa_v, \kappa_r)$, we use the following analysis based on the method of Han *et al.* (1999).

Firstly, let Eq. (29) with a given s be $F(a, \kappa_v, \kappa_r)=0$. Setting $\kappa_r=0$ yields $H_1(a, \kappa_v)=F(a, \kappa_v, \kappa_r=0)$, then $\mathrm{d}H_1$ can be given by

$$\mathrm{d}H_1 = \frac{\partial H_1}{\partial a}\mathrm{d}a + \frac{\partial H_1}{\partial \kappa_v}\mathrm{d}\kappa_v \tag{30}$$

in which $\mathrm{d}H_1$ is zero because F is zero. Solving for $\mathrm{d}a/\mathrm{d}\kappa_v$, we obtain

$$\frac{\mathrm{d}a}{\mathrm{d}\kappa_v} = -\frac{\partial H_1}{\partial \kappa_v}\Big/\frac{\partial H_1}{\partial a} \tag{31}$$

The right-hand side of the above equation is a function of a and κ_v only. This is a first-order ordinary differential equation which can be solved once we know the initial value $a(\kappa_v=0, \kappa_r=0)$. $\kappa_v=\kappa_r=0$ means omitting the effects of elastic constraints, then Eq. (29) becomes "$1+\cos a\cosh a=0$" whose solutions have been tabulated in many papers and books, such as the book of (Young and Felgar 1949). Using these existing results as the initial values, we can obtain a smooth function of $a(\kappa_v, \kappa_r=0)$.

Then Setting κ_v to be an arbitrary constant κ_{vc} ($\kappa_{vc} \geq 0$) results in $H_2(a, \kappa_r)=F(a, \kappa_v=\kappa_{vc}, \kappa_r)$. In the same way, we can obtain

$$\mathrm{d}H_2 = \frac{\partial H_2}{\partial a}\mathrm{d}a + \frac{\partial H_2}{\partial \kappa_r}\mathrm{d}\kappa_r \tag{32}$$

and

$$\frac{\mathrm{d}a}{\mathrm{d}\kappa_r} = -\frac{\partial H_2}{\partial \kappa_r}\Big/\frac{\partial H_2}{\partial a} \tag{33}$$

Similarly the right-hand side of Eq. (33) is a function of a and κ_r. This is also a first-order ordinary differential equation which can be solved once we know the initial value $a(\kappa_v=\kappa_{vc}, \kappa_r=0)$

which has been obtained ahead. Moreover, κ_{vc} is arbitrary, so we can calculate the wave number a at any point ($\kappa_v \geq 0$, $\kappa_r \geq 0$). So far, we have obtained a smooth solution $a(\kappa_v, \kappa_r)$ for Eq. (29).

It should be noted here that the above analysis is just to obtain the formulae of $\mathrm{d}a/\mathrm{d}\kappa_v$ and $\mathrm{d}a/\mathrm{d}\kappa_r$. However, it is difficult or impossible to derive the analytical solution for $a(\kappa_v, \kappa_r=0)$ or $a(\kappa_v=\kappa_{vc}, \kappa_r)$, from the formula of $\mathrm{d}a/\mathrm{d}\kappa_v$ or $\mathrm{d}a/\kappa_r$. So this method is essentially a numerical one. Using this method, we can calculate the solution of $a(\kappa_v, \kappa_r)$ along a line, one by one from the initial value point.

5. Mode shape functions

After solving for the wave number, the mode shape function, Eq. (27), corresponding to the obtained wave number can be determined. For each root of the wave number, there exists one mode shape of vibration which can be obtained as follows.

Any three of the four coefficients c_n (n=1, 2, 3, 4) in Eq. (27) can be solved by three liner algebraic equations in Eq. (28). Here we solve c_1, c_2 and c_3 from the first three equations. By elementary transformation we obtain

$$c_1 = \frac{\alpha_1}{\alpha_0} c_4,\ c_2 = -\frac{\alpha_2}{\alpha_0} c_4,\ c_3 = -\frac{\alpha_3}{\alpha_0} c_4 \tag{34}$$

in which

$$\begin{aligned}
\alpha_0 &= (1-\kappa_v\kappa_r r^2 a^4)\sin a + (1+\kappa_v\kappa_r r^2 a^4)\sinh a + 2\kappa_v r^2 a^3 \cos a \\
\alpha_1 &= (1-\kappa_v\kappa_r r^2 a^4)\cosh a + (1+\kappa_v\kappa_r r^2 a^4)\cos a + 2\kappa_r a \sinh a \\
\alpha_2 &= (1-\kappa_v\kappa_r r^2 a^4)\sinh a + (1+\kappa_v\kappa_r r^2 a^4)\sin a - 2\kappa_v r^2 a^3 \cosh a \\
\alpha_3 &= (1-\kappa_v\kappa_r r^2 a^4)\cos a + (1+\kappa_v\kappa_r r^2 a^4)\cosh a - 2\kappa_r a \sin a
\end{aligned}$$

Then the shape function becomes

$$\begin{aligned}
V(\xi) = \frac{c_4}{\alpha_0}\Big[&\alpha_1 \sin a\xi - \alpha_2 \cos a\xi - \alpha_3 \sinh a\xi + \alpha_0 \cosh a\xi - (\alpha_1+\alpha_3)\kappa_v r^2 a^3 \\
&- (\alpha_0+\alpha_2)\kappa_r a^2 \xi\Big]
\end{aligned} \tag{35}$$

where c_4 should be no-zero to represent vibration amplitude.

Clearly, Eq. (35) is valid when α_0 is non-zero. If α_0=0, the shape function may be obtained by solving the coefficients c_1, c_2 and c_4 from the first two linear algebraic equations plus the fourth one in Eq. (28), thus we can obtain the shape function as

$$\begin{aligned}
V(\xi) = \frac{c_3}{\beta_0}\Big[&\beta_1 \sin a\xi - \beta_2 \cos a\xi + \beta_0 \sinh a\xi + \beta_3 \cosh a\xi - (\beta_1-\beta_0)\kappa_v r^2 a^3 \\
&- (\beta_2+\beta_3)\kappa_r a^2 \xi\Big]
\end{aligned} \tag{36}$$

in which

$$\beta_0 = (1-\kappa_v\kappa_r r^2 a^4)\sin a - (1+\kappa_v\kappa_r r^2 a^4)\sinh a + 2\kappa_r a\cos a$$
$$\beta_1 = (1-\kappa_v\kappa_r r^2 a^4)\sinh a - (1+\kappa_v\kappa_r r^2 a^4)\sin a + 2\kappa_r a\cosh a$$
$$\beta_2 = (1-\kappa_v\kappa_r r^2 a^4)\cosh a + (1+\kappa_v\kappa_r r^2 a^4)\cos a - 2\kappa_v r^2 a^3\sinh a$$
$$\beta_3 = (1-\kappa_v\kappa_r r^2 a^4)\cos a + (1+\kappa_v\kappa_r r^2 a^4)\cosh a - 2\kappa_v r^2 a^3\sin a$$

As shown in Eqs. (35) and (36), for each root of the wave number, the coefficients c_n (n=1, 2, 3, 4) in Eq. (27) are unique to a constant c_4 or c_3. For convenience, the remaining constant in the eigenfunction is usually determined by normalization. Here we use the following formula to normalize Eqs. (35) and (36).

$$\max|V(\xi)|=1 \tag{37}$$

6. Results and discussions

The initial value problems shown in Section 4 are solved using MATLAB, and the results will be shown and discussed in this section. Table 1 shows the first five wave numbers a_n (n=1, 2, …, 5) of the cantilever beam with rigid constraints from Young and Felgar (1949), which will be used as initial values in the calculations. As shown in Table 1, for the Bernoulli-Euler beam with rigid constraints, the wave number a is independent of the slenderness ratio s. However, for the Bernoulli-Euler beam with elastic constraints, a depends upon s when $\kappa_v\neq0$, as shown by Eq. (29). When κ_v=0, Eq. (29) degenerates into

$$(1+\cos a\cosh a) - \kappa_r a(\sin a\cosh a - \cos a\sinh a) = 0 \tag{38}$$

Clearly, there is no s in the above equation, so a is independent of s when κ_v=0. In order to represent the effects of slenderness ratio when $\kappa_v\neq0$, four cases are taken into account in this study, i.e., s=100, 50, 30, 20. Besides, the beam theory in this paper is based on the assumption of small displacement, so κ_v and κ_r cannot be very large from a practical point of view. Here, the ranges of κ_v and κ_r are both set as [0,5].

6.1 Natural frequencies

First of all, let us consider the natural frequency or wave number a. Figs. 3(a)-(d) show the three-dimensional change surfaces of the first five wave numbers a_n (n=1, 2, …, 5) with κ_v and κ_r when s=100, 50, 30 and 20, respectively. Obviously, elastic constraints soften the beam, i.e., reduce the wave numbers. It can be concluded qualitatively from Fig. 3 that the effects of elastic constraints on the wave numbers, i.e., the reduction of a, increase with the increase of κ_v and κ_r, and decrease with the increase of the slenderness ratio s when $\kappa_v\neq0$. κ_v and κ_r have very different effects on the wave number. The effects of κ_r on the first-order wave number a_1 are larger than those of κ_v,

Table 1 The first five wave numbers of the cantilever beam when $\kappa_v=\kappa_r=0$ (Young and Felgar 1949)

s	a_1	a_2	a_3	a_4	a_5
100,50,30,20	1.8751041	4.69409113	7.85475743	10.99554074	14.13716839

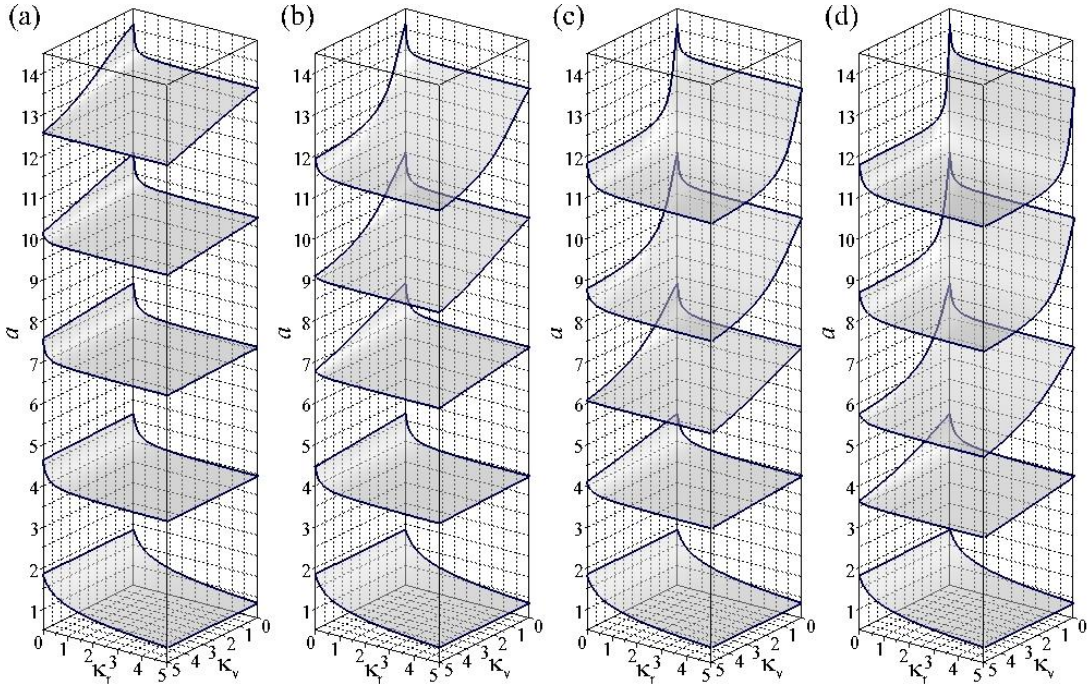

Fig. 3 Variations of the first five wave numbers a_n (n=1, 2, …, 5) with κ_v and κ_r: (a) s=100, (b) s=50, (c) s=30 and (d) s=20

and are almost the same for different slenderness ratios. Whereas, the effects of κ_v on higher-order wave numbers, such as a_5, are larger than those of κ_r especially when s is small. Besides, higher-order wave numbers are more sensitive to a small κ_v or a small κ_r, while are insensitive to a large κ_v or a large κ_r.

In order to give an obviously quantitative comparison, Fig. 4 shows the variations of the first five wave numbers with κ_v when κ_r=0, 0.1, 1, and 5, and Fig. 5 shows the variations of the first five wave numbers with κ_r when κ_v=0, 1, 3, and 5. Clearly, as shown in Fig. 4, the effects of κ_v and κ_r increase with not only the increase of κ_v and κ_r but also the decrease of s. Moreover, the sensitivity of wave number to κ_v (or the absolute reduction of the wave number) increases with the order number. Higher-order wave numbers are very sensitive to a small κ_v especially when s is small, while are insensitive to a large κ_v. As shown in Fig. 4d for s=20, when κ_r =0, from κ_v=0 to 1 and to 5, the wave number a_5 varies from 14.137 to 11.914 (cut by −15.7%) and to 11.806 (cut by −16.5%). However, the first-order wave number a_1 is nearly independent of κ_v even for a small s. Also in Fig. 4(d), when κ_r=0, from κ_v=0 to 1 and to 5, a_1 varies from 1.8751 to 1.8662 (cut by −0.5%) and to 1.8309 (cut by −2.4%). So the effects of κ_v can generally be neglected for a_1, while cannot for high-order wave numbers even under a large s as shown in Fig. 4(a).

Turn to Fig. 5. Clearly, when κ_v=0, a is independent of κ_r, the reason for which has been stated in the beginning of this section. Besides when κ_v=0, variations of the second- to fifth-order wave numbers are almost the same for all considered slenderness ratios, and are sensitive to a small κ_r. However, with increase of κ_v, the variation shapes change greatly. For certain values of κ_v, the wave number is nearly independent of κ_r. As shown in Fig. 5(b), when κ_v=3, a_4 is equal to a constant 9.4212 as κ_r varies from 0 to 5. The effects of κ_r on the first-order wave number a_1 are

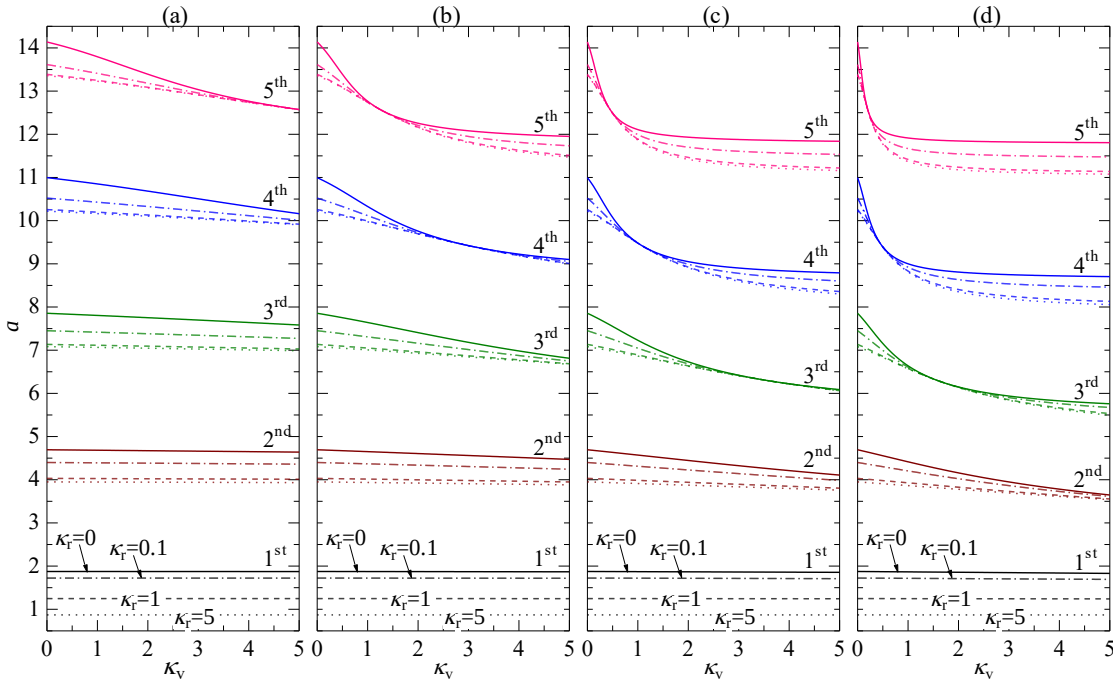

Fig. 4 Variations of the first five wave numbers a_n (n=1, 2, …, 5) with κ_v when κ_r=0, 0.1, 1 and 5: (a) s=100, (b) s=50, (c) s=30 and (d) s=20

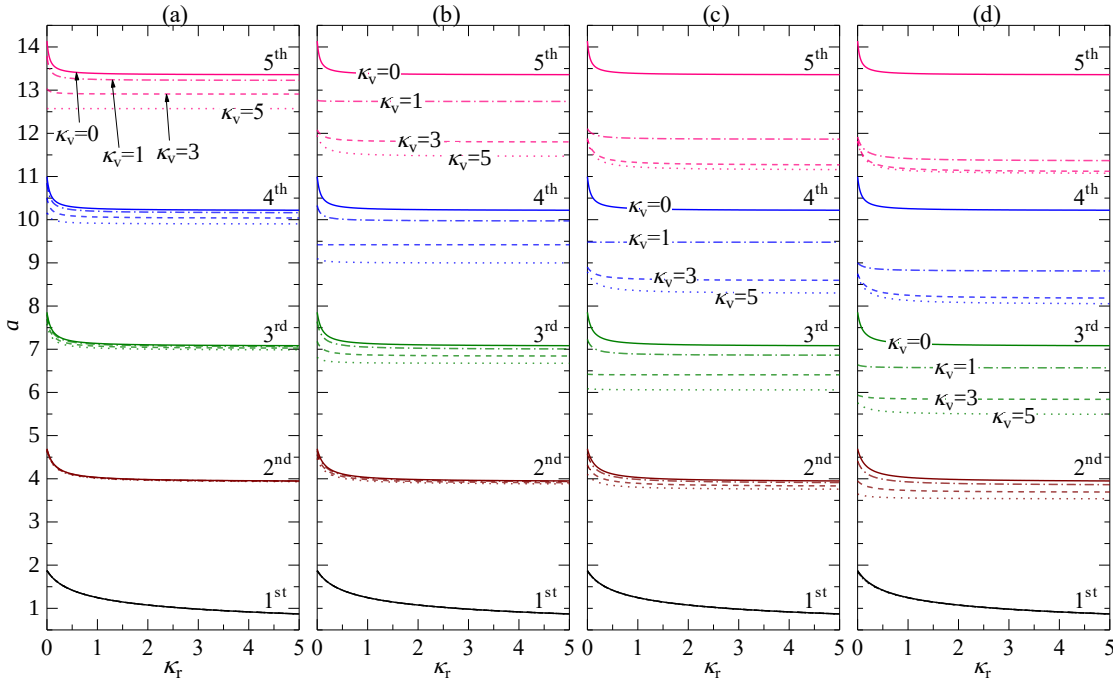

Fig. 5 Variations of the first five wave numbers a_n (n=1, 2, …, 5) with κ_r when κ_v=0, 1, 3 and 5: (a) s=100, (b) s=50, (c) s=30 and (d) s=20

obvious, different from the effects of κ_v shown in Fig. 4, and are nearly independent of κ_v no matter s is large or small. As shown in Fig. 5a for s=100, when κ_v=0, from κ_r=0 to 1 and to 5, a_1 varies from 1.8751 to 1.2479 (cut by −33.4%) and to 0.8700 (cut by −53.6%). So the effects of κ_r cannot be neglected for all considered cases.

6.2 Mode shapes

Substituting the obtained wave numbers in the above subsection into Eqs. (35) or (36) yields the corresponding mode shapes. Figs. 6-7 show the variations of the first five mode shapes with κ_v and κ_r under s=100 and 20, respectively. To facilitate comparison, the mode shapes of the beam with rigid constraints, i.e., κ_r=κ_v=0.00, are also shown in the figures. All mode shapes are normalized using Eq. (37). Clearly κ_v and κ_r have great effects on all considered mode shapes except the first-order one although the first-order wave number depends strongly upon κ_r as shown in Fig. 5. Similar to the wave number, effects of κ_v and κ_r on mode shapes increase with the increase of κ_v and κ_r until to some certain values above which the mode shapes are insensitive to their changes. When κ_v=0, mode shapes are independent of the slenderness ratio as shown in Figs. 6(a) and 7(a), but when $\kappa_v\neq$0, effects of κ_v and κ_r on mode shapes increase with the increase of s and the order number. Besides, we can also find by comparing Fig. 6(c) with Fig. 7(c) (or Fig. 6(d) with Fig. 7(d)) that when s is small, i.e., s=20, the fourth- and fifth-order mode shapes have degenerated into the third- and fourth-order ones, respectively for κ_r=0.20, 2.00 (or κ_v =1.50, 5.00) and for κ_v=0.70 (or κ_r =0.04).

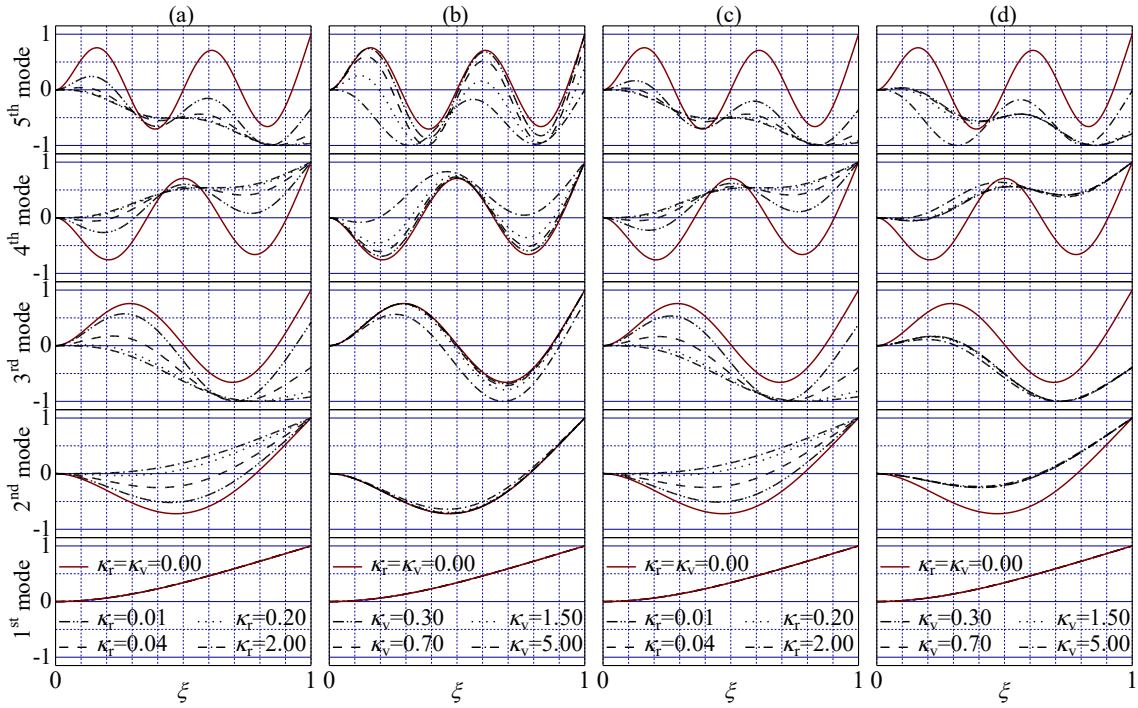

Fig. 6 Variations of the first five mode shapes $V(\xi)$ with κ_v and κ_r under s=100: (a) κ_v=0.00, (b) κ_r=0.00, (c) κ_v=0.70 and (d) κ_r=0.04

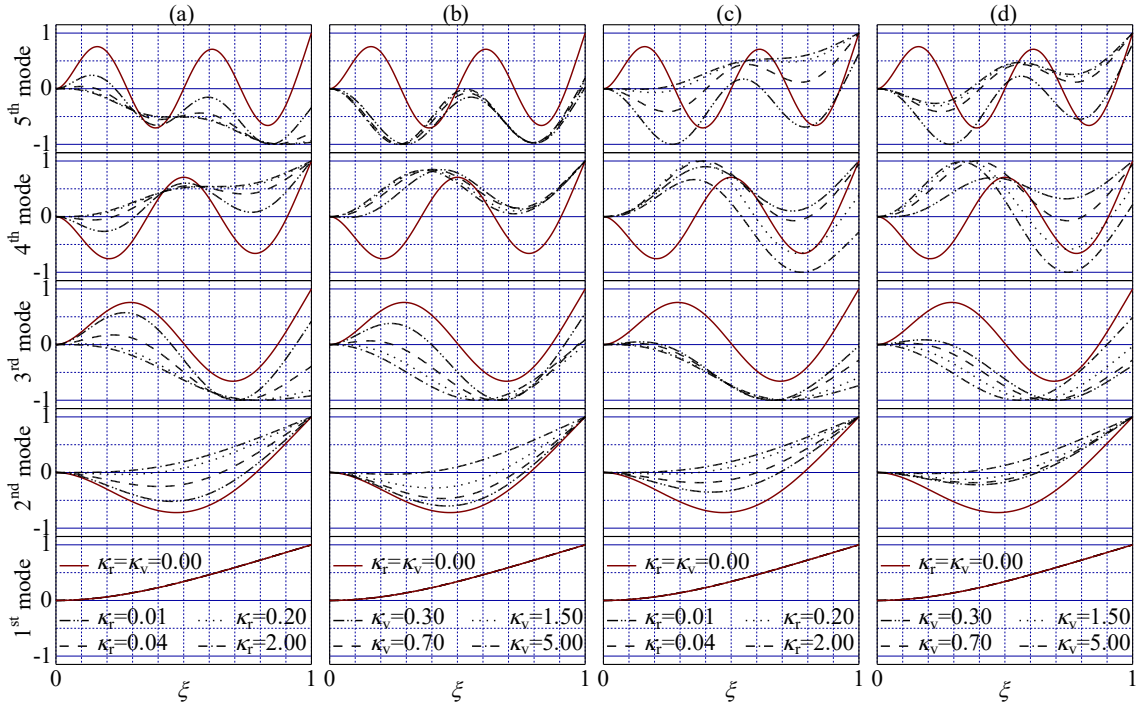

Fig. 7 Variations of the first five mode shapes $V(\xi)$ with κ_v and κ_r under s=20: (a) κ_v=0.00, (b) κ_r=0.00, (c) κ_v=0.70 and (d) κ_r=0.04

7. Conclusions

In this paper, we established the equation of motion governing the cantilever Bernoulli-Euler beams considering the deformation of elastic constraints, and the corresponding frequency equation and mode shape functions were also given. An analysis-based numerical method was proposed to solve the frequency equation. Finally, effects of elastic constraints on free vibration characteristics of the beam were calculated and analyzed. The following conclusions can be suggested:

- The governing equation of motion for the uniform cantilever Bernoulli-Euler beam was established considering the deformation of elastic constraints, and was nondimensionalized to obtain two factors, κ_v and κ_r, respectively controlling the elastically vertical and rotational end constraints.
- The frequency equation and mode shape functions corresponding to the above beam model were derived in detail. If κ_v=0, the frequency equation is independent of the slenderness ratio, or in other words, the frequency will not change with the slenderness ratio when κ_v =0.
- In order to obtain the continuous change of the frequency or wave number with κ_v and κ_r, an analysis-based numerical method given by Han *et al.* (1999) was used to solve the transcendental frequency equation.
- Effects of κ_v and κ_r on natural frequencies or wave numbers increase with the increase of κ_v and κ_r until to some certain values above which the frequencies are insensitive to their changes. Higher-order frequencies are very sensitive to a small κ_v or a small κ_r, and a small s increases

the sensitivity. The first-order frequency is nearly independent of κ_v and the slenderness ratio, while strongly depends upon κ_r.

• Effects of κ_v and κ_r on mode shapes are similar to those on wave numbers except that the first-order mode shape is insensitive to with κ_r while the first-order wave number depends strongly upon κ_r. Besides, when the slenderness ratio is relatively small, with increase of κ_v and κ_r, the nth-order mode shape may change into the $(n-1)$th-order one.

Acknowledgments

This research was financially supported by the National Natural Science Foundation of China (Grant No. 51508333 and 51508332) and the Innovation Program of Shanghai Municipal Education Commission (Grant No. 14ZZ129).

References

Afolabi, D. (1986), "Natural frequencies of cantilever blades with resilient roots", *J. Sound Vib.*, **110**(3), 429-441.

Choi, H.S. (2001), "Free spanning analysis of offshore pipelines", *Ocean Eng.*, **28**(10), 1325-1338.

Chun, K.R. (1972), "Free vibration of a beam with one end spring-hinged and the other free", *J. Appl. Mech.*, **39**(4), 1154-1155.

Duy, H.T., Van, T.N. and Noh, H.C. (2014), "Eigen analysis of functionally graded beams with variable cross-section resting on elastic supports and elastic foundation", *Struct. Eng. Mech.*, **52**(5), 1033-1049.

Faires, J.D. and Burden, R.L. (2012), *Numerical Methods*, 4th edition, Books Cole, Boston, USA.

Han, S.M., Benaroya, H. and Wei, T. (1999), "Dynamics of transversely vibrating beams using four engineering theories", *J. Sound Vib.*, **225**(5), 935-988.

Kang, J.H. (2014), "An exact frequency equation in closed form for Timoshenko beam clamped at both ends", *J. Sound Vib.*, **333**(14), 3332-3337.

Lee, S.Y. and Ke, H.Y. (2000), "Free vibrations of a non-uniform beam with general elastically restrained boundary conditions", *J. Sound Vib.*, **136**(3), 425-437.

Li, W.L. (2000), "Free vibrations of beams with general boundary conditions", *J. Sound Vib.*, **237**(4), 709-725.

Liang, X., Hu, S. and Shen, S. (2014), "A new Bernoulli-Euler beam model based on a simplified strain gradient elasticity theory and its applications", *Compos. Struct.*, **111**(11), 317-323.

Maurizi, M.J., Rossi, R.E. and Reyes, J.A. (1976), "Vibration frequencies for a beam with one end spring hinged and subjected to a translational restraint at the other end", *J. Sound Vib.*, **48**(4), 565-568.

Ozturk, B. and Coskun, S.B. (2013), "Analytical solution for free vibration analysis of beam on elastic foundation with different support conditions", *Math. Probl. Eng.*, Article ID 470927, 1-7.

Plankis, A., Lebsack, M. and Heyliger, P.R. (2015), "Elasticity-based beam vibrations for various support conditions", *Appl. Math. Model.*, **39**(22), 6860-6879.

Rao, C.K. and Mirza, S. (1989), "A note on vibrations of generally restrained beams", *J. Sound Vib.*, **130**(3), 453-465.

Shi, L., Yan, W. and He, H. (2014), "The modal characteristics of non-uniform multi-span continuous beam bridges", *Struct. Eng. Mech.*, **52**(5), 997-1017.

Thomson, W.T. and Dahleh, M.D. (1997), *Theory of Vibration with Applications*, 5th Edition, Prentice Hall, Upper Saddle River, New Jersey, USA.

Timoshenko, S.P. (1953), *History of Strength of Materials*, Dover Publications, Inc., New York, USA.

Traill-Nash, R.W. and Collar, A.R. (1953), "The effects of shear flexibility and rotatory inertia on the

bending vibrations of beams", *Q. J. Mech. Appl. Math.*, **6**(2), 186-222.
Wang, T., Li, H. and Ge, Y. (2015), "Vertical seismic response analysis of straight girder bridges considering effects of support structures", *Earthq. Struct.*, **8**(6), 1481-1497.
Xing, J.Z. and Wang, Y.G. (2013), "Free vibrations of a beam with elastic end restraints subject to a constant axial load", *Arch. Appl. Mech.*, **83**(2), 241-252.
Young, D. and Felgar, R.P. (1949), *Tables of Characteristic Functions Representing Normal Modes of Vibration of a Beam*, The University of Texas Press, Austin, USA.

CC